

See discussions, stats, and author profiles for this publication at: <https://www.researchgate.net/publication/23758852>

# Protein-Directed Synthesis of Highly Fluorescent Gold Nanoclusters

ARTICLE in JOURNAL OF THE AMERICAN CHEMICAL SOCIETY · FEBRUARY 2009

Impact Factor: 12.11 · DOI: 10.1021/ja806804u · Source: PubMed

---

CITATIONS

728

---

READS

1,067

3 AUTHORS, INCLUDING:



Jianping Xie

National University of Singapore

109 PUBLICATIONS 4,346 CITATIONS

SEE PROFILE



Yuangang Zheng

Agency for Science, Technology and Resea...

37 PUBLICATIONS 2,196 CITATIONS

SEE PROFILE

## Protein-Directed Synthesis of Highly Fluorescent Gold Nanoclusters

Jianping Xie, Yuangang Zheng, and Jackie Y. Ying\*

Institute of Bioengineering and Nanotechnology, 31 Biopolis Way, The Nanos, Singapore 138669

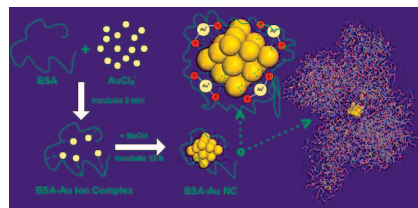
Received August 28, 2008; E-mail: jyying@ibn.a-star.edu.sg

Noble metal nanoclusters (NCs) typically consist of several to tens of atoms. They are <1 nm in size, and their properties are governed by their subnanometer dimensions.<sup>1</sup> This size regime is comparable to the Fermi wavelength of the conduction electrons. The spatial confinement of free electrons in metal nanoclusters results in discrete and size-tunable electronic transitions, leading to molecular-like properties such as luminescence and unique charging properties.<sup>1</sup> In contrast to semiconductor quantum dots (QDs), which are larger in dimensions (~3 to 100 nm) and typically contain toxic metal species (e.g., cadmium, lead),<sup>2–6</sup> noble metal NCs are highly attractive for biolabeling and bioimaging applications because of their ultrafine size and nontoxicity.

Thiol-protected Au NCs that consist of several to a hundred atoms (<1.2 nm) have been synthesized previously via chemical reduction (e.g., with sodium borohydride (NaBH<sub>4</sub>)) of Au precursors in the presence of thiols (e.g., glutathione).<sup>7–11</sup> While these Au NCs fluoresce in the blue to near-IR regimes, the quantum yields (QYs) are relatively low (0.001%–0.1%). Recently, Au NCs with >10% QY have been prepared using a poly(amidoamine) dendrimer as template.<sup>1,12</sup> However, this synthesis<sup>1,12–15</sup> requires a fairly long reaction time (~2 days) and produces large nanoparticles as byproduct. Nie and Duan have reported a ligand-induced (poly-ethylenimine) etching process for the synthesis of highly fluorescent Au NCs with blue emission.<sup>13</sup> It would be of great interest to derive highly fluorescent Au NCs with red or near-infrared emissions that offer improved tissue penetration depth and reduced background fluorescence.

Herein, we reported a simple, one-pot, “green” synthetic route, based on the capability of a common commercially available protein, bovine serum albumin (BSA), for the preparation of Au NCs at the physiological temperature (37 °C) with red emission ( $\lambda_{\text{em max}} = 640$  nm, QY  $\approx$  6%). Our process is similar to the biomineralization behavior of organisms in nature: sequestering and interacting with inorganic ions, followed by providing scaffolds for minerals formed, mostly through functional proteins. We showed that upon adding Au(III) ions to the aqueous BSA solution, the protein molecules sequestered Au ions and entrapped them (see Scheme 1). The reduction ability of BSA molecules was then activated by adjusting the reaction pH to  $\sim$ 12; the entrapped ions underwent progressive reduction to form Au NCs in situ. The as-prepared Au NCs consisted of 25 gold atoms and were stabilized within BSA molecules as BSA–Au NC bioconjugates. Besides the good biocompatibility and considerable environmental/cost advantages of this methodology, the BSA coating layer on Au NCs also facilitated postsynthesis surface modifications with functional ligands.

BSA, the most abundant plasma protein widely used in applications such as sensing, self-assembly, and imaging,<sup>16</sup> was selected as the model protein for the synthesis of Au NCs. It was recently used to stabilize Au particles of nm to  $\mu$ m in dimensions.<sup>17</sup> Herein BSA was employed in the preparation of subnanometer-sized clusters. In a typical experiment, aqueous HAuCl<sub>4</sub> solution (5 mL,

**Scheme 1.** Schematic of the Formation of Au NCs in BSA Solution

10 mM, 37 °C) was added to BSA solution (5 mL, 50 mg/mL, 37 °C) under vigorous stirring. Two minutes later, NaOH solution (0.5 mL, 1 M) was introduced, and the mixture was incubated at 37 °C for 12 h. The color of the solution changed from light yellow to light brown, and then to deep brown (Figure 1a, top item no. 3). The reaction was completed in  $\sim$ 12 h, as confirmed by time-course measurements of the fluorescence evolution (Supporting Information, Figure S1).

The deep brown solution of Au NCs emitted an intense red fluorescence (Figure 1a, bottom item no. 3) under UV light (365 nm). In contrast, the control BSA solution was pale yellow in color under visible light (Figure 1a, top item no. 2) and emitted a weak blue fluorescence under UV light (Figure 1a, bottom item no. 2), which was characteristic of the aromatic side groups in the amino acid residues (tryptophan, tyrosine (Tyr) and phenylalanine). The fluorescent Au NCs showed excitation and emission peaks at 480 and 640 nm, respectively (Figure 1b). The photoluminescence QY was  $\sim$ 6% (calibrated with fluorescein using a 470-nm laser). To our knowledge, this was the first successful attempt on “green” chemical synthesis of highly fluorescent Au NCs with red emissions.

The oxidation state of the Au NCs was determined by X-ray photoelectron spectroscopy (XPS). The Au 4f<sub>7/2</sub> spectrum could be deconvoluted into two distinct components (red and blue curves) centered at binding energies of 84.0 and 85.1 eV, which could be assigned to Au(0) and Au(I), respectively (Figure 2a). The small amount of Au(I) ( $\sim$ 17%) present on the surface of the Au core

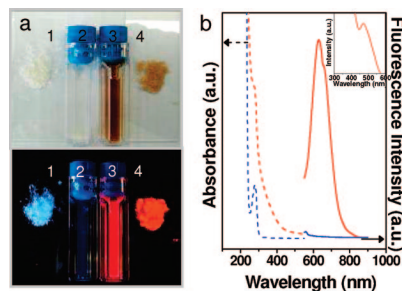


**Figure 1.** (a) Photographs of BSA (1) powder and (2) aqueous solution, and BSA–Au NCs (3) aqueous solution and (4) powder under (top) visible and (bottom) UV light. (b) Optical absorption (dash lines) and photoemission (solid lines,  $\lambda_{\text{ex}} = 470$  nm) spectra of aqueous solution of (blue) BSA and (red) BSA–Au NCs. The inset shows the photoexcitation spectrum of BSA–Au NCs.

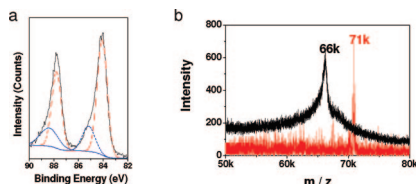


**Figure 2.** (a) XPS spectra of Au 4f for BSA–Au NCs (black); (b) MALDI-TOF mass spectra of BSA (black) and BSA–Au NCs (red).

helped to stabilize the NCs (see Scheme 1), as noted in a structural study of thiol-protected Au NCs.<sup>18,19</sup> The as-prepared BSA–Au NCs might have a similar structure considering the presence of 35 thiol groups (from the 35 cysteine (Cys) residues) in a BSA monomer. The Au NCs have a photoemission peak at  $\sim 640$  nm, indicating the presence of Au<sub>25</sub> clusters based on the spherical Jellium model.<sup>12</sup> Matrix-assisted laser desorption/ionization-time-of-flight (MALDI-TOF) mass spectrometry<sup>20</sup> showed the BSA molecular weight to be  $\sim 66$  kDa (Figure 2b). The as-prepared BSA–Au NCs showed a peak shift of  $\sim 5$  kDa, which could be attributed to the 25 gold atoms in the Au NCs. Thermal gravimetric (TGA) analysis of BSA–Au NCs also provided a supporting evidence (Figure S2). Au NC with 25 atoms has been reported to have a highly stable structure,<sup>21</sup> and corresponded to the most common magic cluster size.<sup>7–11</sup>

No obvious change in fluorescence properties was observed for BSA–Au NCs in solutions of a broad pH range (3–12), in various buffer solutions (e.g., 50 mM of HEPES buffer (pH 7.65)), or in solutions with a high salt concentration (e.g., 1 M NaCl). The solvent could be removed by freeze-drying, and the BSA–Au NCs could be stored in the solid form (Figure 1a, item no. 4) for at least 2 months and redispersed when needed. The Au NCs formed in the BSA solution could have been stabilized by a combination of Au–S bonding with the protein (via the 35 Cys residues in BSA), and the steric protection due to the bulkiness of the protein. The high stability of BSA–Au NCs would greatly facilitate their use in *in vitro* and *in vivo* bioimaging applications. The encapsulation of Au NCs ( $\sim 0.8$  nm) (Figure S3) in BSA molecules has little effect on the structure of the BSA scaffolds (see Figure S4).

While it was not clear at the molecular level how BSA “biomineralized” the highly fluorescent Au NCs, there were several revealing observations: (i) Both the *in situ* reduction of encapsulated Au ions by the responsible residues of protein and the addition of NaOH were important. Control experiments were performed by adding an extraneous reductant, NaBH<sub>4</sub>, in the same reaction solution as for the BSA–Au NCs synthesis. The resulting BSA–Au NCs emitted very weak red fluorescence (QY  $\approx 0.1\%$ , Table S1 and Figure S5). Recent studies have shown that Tyr or custom peptides containing Tyr residues can reduce Au(III) or Ag(I) ions through their phenolic groups; their reduction capability can be greatly improved by adjusting the reaction pH above the pK<sub>a</sub> of Tyr ( $\sim 10$ ).<sup>22</sup> Hence, the reducing capability of BSA was not unexpected since it contains 21 Tyr residues and possibly other residues with reduction functionality. The addition of NaOH was also necessary, without which only large nanoparticles ( $> 20$  nm) with irregular or plate-like morphologies were obtained (Figure S6), and these nanoparticles showed no fluorescence (Figure S5). (ii) The reaction temperature was an important consideration in the synthesis of fluorescent Au NCs. It was found that Au NCs formed very slowly at 25 °C; no clusters were detected even after 12 h of reaction. Reactions at the physiological temperature (37 °C) showed

reasonable reduction kinetics. Reaction was completed within 12 h, and Au NCs with high QYs ( $\sim 6\%$ ) were obtained. When conducted at 100 °C, the reaction was completed within minutes; however, the as-prepared Au NCs have relatively low QY ( $\sim 0.5\%$ ) (Table S1 and Figure S5). (iii) The concentrations of BSA and Au precursors were critical. At a fixed Au precursor concentration (5 mM), a high BSA concentration (10–25 mg/mL) (with a concentration of amino acid residues of  $\sim 20$  to 50 mM) was required for the effective protection of Au NCs. Decreasing the BSA concentration to 2.5 mg/mL, while keeping Au precursor concentration constant (5 mM), would produce large nanoparticles with no fluorescence (Table S1 and Figure S5).

In summary, we have developed a new method for preparing Au NCs with red emissions using a common protein to sequester and reduce Au precursors *in situ*. The as-prepared BSA–Au NCs are highly stable both in solutions (aqueous or buffer) and in the solid form. The light-emitting Au NCs consist of 25 gold atoms (Au<sub>25</sub>). The experimental conditions have been optimized to derive Au NCs with high QYs. The protocols and products are important not only because they provide a simple, “green” method for the production of highly fluorescent Au NCs, but also because they exemplify that the interactions between proteins/peptides and Au ions (biomineralization or biomimetic mineralization) can be used toward the creation of protein–Au NC bioconjugates. The synthesis protocol is expected to be applicable to other proteins and noble metals (e.g., Ag).

**Acknowledgment.** The authors acknowledge helpful discussions with Prof. Jim Yang Lee. This work is funded by the Institute of Bioengineering and Nanotechnology (Biomedical Research Council, Agency for Science, Technology and Research, Singapore).

**Supporting Information Available:** Experimental details of the synthesis and characterization of materials. This material is available free of charge via the Internet at <http://pubs.acs.org>.

## References

- (1) Zheng, J.; Nicovich, P. R.; Dickson, R. M. *Annu. Rev. Phys. Chem.* **2007**, *58*, 409.
- (2) Zheng, Y.; Gao, S.; Ying, J. Y. *Adv. Mater.* **2007**, *19*, 376.
- (3) Zheng, Y.; Yang, Z.; Ying, J. Y. *Adv. Mater.* **2007**, *19*, 1475.
- (4) Michalet, X.; Pinaud, F. F.; Bentolila, L. A.; Tsay, J. M.; Doose, S.; Li, J. J.; Sundaresan, G.; Wu, A. M.; Gambhir, S. S.; Weiss, S. *Science* **2005**, *307*, 538.
- (5) Nie, S. M.; Xing, Y.; Kim, G. J.; Simons, J. W. *Annu. Rev. Biomed. Eng.* **2007**, *9*, 257.
- (6) Hardman, R. *Environ. Health Perspect.* **2006**, *114*, 165.
- (7) Negishi, Y.; Chaki, N. K.; Shichibu, Y.; Whetten, R. L.; Tsukuda, T. *J. Am. Chem. Soc.* **2007**, *129*, 11322.
- (8) Negishi, Y.; Nobusada, K.; Tsukuda, T. *J. Am. Chem. Soc.* **2005**, *127*, 5261.
- (9) Negishi, Y.; Takasugi, Y.; Sato, S.; Yao, H.; Kimura, K.; Tsukuda, T. *J. Am. Chem. Soc.* **2004**, *126*, 6518.
- (10) Shichibu, Y.; Negishi, Y.; Tsunoyama, H.; Kanehara, M.; Teranishi, T.; Tsukuda, T. *Small* **2007**, *3*, 835.
- (11) Wang, G. L.; Huang, T.; Murray, R. W.; Menard, L.; Nuzzo, R. G. *J. Am. Chem. Soc.* **2005**, *127*, 812.
- (12) Zheng, J.; Zhang, C. W.; Dickson, R. M. *Phys. Rev. Lett.* **2004**, *93*, 4.
- (13) Duan, H. W.; Nie, S. M. *J. Am. Chem. Soc.* **2007**, *129*, 2412.
- (14) Lee, W. I.; Bae, Y. J.; Bard, A. J. *J. Am. Chem. Soc.* **2004**, *126*, 8358.
- (15) Tran, M. L.; Zvyagin, A. V.; Plakhotnik, T. *Chem. Commun.* **2006**, 2400.
- (16) Tkachenko, A. G.; Xie, H.; Coleman, D.; Glomm, W.; Ryan, J.; Anderson, M. F.; Franzen, S.; Feldheim, D. L. *J. Am. Chem. Soc.* **2003**, *125*, 4700.
- (17) Xie, J.; Lee, J. Y.; Wang, D. I. C. *J. Phys. Chem. C* **2007**, *111*, 10226.
- (18) Whetten, R. L.; Price, R. C. *Science* **2007**, *318*, 407.
- (19) Jazdzinsky, P. D.; Calero, G.; Ackerson, C. J.; Bushnell, D. A.; Kornberg, R. D. *Science* **2007**, *318*, 430.
- (20) Scott, D.; Toney, M.; Muzikar, M. *J. Am. Chem. Soc.* **2008**, *130*, 865.
- (21) Zhu, M.; Aikens, C. M.; Hollander, F. J.; Schatz, G. G.; Jin, R. *J. Am. Chem. Soc.* **2008**, *130*, 5883.
- (22) Xie, J.; Lee, J. Y.; Wang, D. I. C.; Ting, Y. P. *ACS Nano* **2007**, *1*, 429.

JA806804U